Acta Oncologica, 2013; 52: 658–665

informa
healthcare

ORIGINAL ARTICLE

Improved tumour control probability with MRI-based prostate brachytherapy treatment planning

ANNA M. DINKLA, BRADLEY R. PIETERS, KEES KOEDOODER, NIEK VAN WIERINGEN, ROB VAN DER LAARSE, JOHAN N. VAN DER GRIENT, COEN R. RASCH, CARO C. KONING & ARJAN BEL

Department of Radiation Oncology, Academic Medical Centre, Amsterdam, the Netherlands

Abstract

Background. Due to improved visibility on MRI, contouring of the prostate is improved compared to CT. The aim of this study was to quantify the benefits of using MRI for treatment planning as compared to CT-based planning for temporary implant prostate brachytherapy. *Material and methods.* CT and MRI image data of 13 patients were used to delineate the prostate and organs at risk (OARs) and to reconstruct the implanted catheters (typically 12). An experienced treatment planner created plans on the CT-based structure sets (CT-plan) and on the MRI-based structure sets (MRI-plan). Then, active dwell-positions and weights of the CT-plans were transferred to the MRI-based structure sets ($\text{CT-plan}_{\text{MRI-contours}}$) and resulting dosimetric parameters and tumour control probabilities (TCPs) were studied. *Results*. For the $\text{CT-plan}_{\text{MRI-contours}}$ a statistically significant lower target coverage was detected: mean V_{100} was 95.1% as opposed to 98.3% for the original plans ($p < 0.01$). Planning on CT caused cold-spots that influence the TCP. MRI-based planning improved the TCPs by 6–10%, depending on the parameters of the radiobiological model used for TCP calculation. Basing the treatment plan on either CT- or MRI-delineations does not influence plan quality. *Conclusion*. Evaluation of CT-based treatment planning by transferring the plan to MRI reveals underdosage of the prostate, especially at the base side. Planning on MRI can prevent cold-spots in the tumour and improves the TCP.

Dose escalation improves biochemical control for intermediate- to high-risk prostate cancer [1]. External beam radiotherapy (EBRT) can be combined with an additional brachytherapy boost to achieve a high dose to the prostate [2]. Stepping source brachytherapy (PDR or HDR) benefits from a steep dose gradient. By adjusting the source dwell times, the treatment plan can be optimised to obtain a conformal high dose in the prostate gland, while sparing the organs at risk (OARs) as much as possible.

Interstitial brachytherapy requires accurate image-based delineation of the boundaries of the prostate and OARs to be able to create treatment plans truly conformal to the target. Accuracy of delineation depends on image quality. It is known that contouring of the prostate on CT images is hampered by lack of soft tissue contrast [3], resulting in suboptimal conformality of the dose distribution to the actual prostate gland. Incorrect delineation of the target volume can result in underdosing the actual target and unnecessary dose to normal tissue. A study by Gao et al. of CT-based prostate contours of six observers showed that despite common overestimation of the prostate, mean overlap was only 84% with their gold standard (high-resolution photographic anatomical images) [4]. It showed that no observer was able to delineate the prostate correctly. MRI overcomes these limitations of CT-based target definition because of better soft tissue differentiation. Visibility of the prostatic apex and prostate boundaries is improved [5] resulting in a reduced inter- and intraobserver variability and the ability to differentiate the seminal vesicles from the dorsal side of the basal edge of the prostate [3,6].

Nowadays CT is still the main modality for treatment planning in stepping source brachytherapy because of existing treatment protocols, availability

Correspondence: A. M. Dinkla, Department of Radiation Oncology, Academic Medical Centre, Meibergdreef 9, 1105 AZ, Amsterdam, the Netherlands. Tel: +31 20 5667992. E-mail: a.m.dinkla@amc.uva.nl

(Received 15 July 2012; accepted 15 October 2012)

ISSN 0284-186X print/ISSN 1651-226X online © 2013 Informa Healthcare
DOI: 10.3109/0284186X.2012.744875

at the department, lower costs and faster image acquisition. On the other hand, MRI provides superior anatomic information [3,5]. A quantification of the actual dosimetric benefits of MRI-based treatment planning for temporary implant brachytherapy, indicating if there is a clinical rationale is not yet available.

We investigated treatment plans based on CT- or MRI-contouring and superimposed the CT-based treatment plans onto the MRI-based delineations to assess the conformity and coverage of dose to the target delineated on MRI. The aim was to investigate whether the use of MRI leads to a significant improvement of the treatment, including the tumour control probability (TCP).

Material and methods

In this planning study 13 patients were included who underwent imaging on two modalities: CT and MRI. On both scans the target and OARs were delineated and catheters were reconstructed for treatment planning. For every patient a CT-based treatment plan and a MRI-based treatment plan were created, hereafter referred to as CT-plan and MRI-plan respectively. The CT-plans were projected on the MRI-datasets, CT-plan$_{\text{MRI-contours}}$, by taking active dwell positions and dwell times from the CT-plans and recalculating the dose on the MRI-based structure set.

Patients and implantation procedure

The 13 patients underwent pulsed-dose rate (PDR) prostate brachytherapy as a boost following EBRT between May 2009 and August 2010. Patients with adverse prognostic factors, such as an initial PSA >10 ng/ml, Gleasonscore ≥ 7, or T2c–T3a, were selected for this treatment, as in our previous studies [7,8]. EBRT (46 Gy/23 fractions) and brachytherapy (28.8 Gy/24 fractions of 1.2 Gy with a period time of 2 hours) was prescribed on the periphery of the prostate. The implantation procedure is described in an earlier study [8]. In brief, 12 flexible 6F catheters (ELLA-CS, Hradec Kralove, Czech Republic) were implanted under ultrasound (US) guidance, according to a preplan. Preplanning was performed intraoperatively with a planning system (Oncentra Prostate, Nucletron, Veenendaal, the Netherlands). The plastic catheters were fixed into the prostate by a self-anchoring mechanism. A transurethral balloon-catheter was introduced into the bladder. Also, three markers, two at the base and one at the apex, were placed to help with the delineation of the prostate boundaries.

Imaging

Within a few hours after implantation, imaging was performed in supine position. A 120 kV helical CT scan (Lightspeed 16 Pro, General Electric, Buc, France) was made with 2.5 mm slices without spacing and an in-plane resolution of 1.17 mm. The reconstruction field of view (FOV) was 60×60 cm^2 with a matrix size of 512×512 pixels. During CT acquisition, patients were given knee support as standard practice at our department for EBRT to represent treatment position. Three orthogonal T2 TSE MRI scans (Avanto Syngo, Siemens, Erlangen, Germany) were acquired with 4 mm slices without interslice gap. Here, spatial resolution was 0.59 mm (30×30 cm^2 FOV, matrix 512×512). During MRI acquisition patients did not receive knee support, since this was not standard practice at the radiology department.

Contouring and treatment planning

Images were loaded into the workstation (Oncentra Brachy vs. 3.2, Nucletron), on which delineation, catheter reconstruction and treatment planning was performed. One experienced radiation oncologist (B.P.) contoured the prostate and base of the seminal vesicles on both the CT and MR images. The prostate and seminal vesicles were considered as the Planning Target Volume (PTV), i.e. without adding a margin. There was no difference in prostate volumes between CT and MRI (Table I, $p = 0.39$). These volumes also did not differ significantly from the pre-implantation volume on US (Table I, $p = 0.3$). The urethra was defined by drawing a circle with 3 mm diameter around the urinary catheter. Rectum and urethra were contoured two slices beyond the

Table I. Prostate volumes (cm^3) as measured on US (during implantation), CT and MRI.

Patient	US	CT	MRI
1	27.2	52.4	30.2
2	49.4	40.1	50.2
3	N/A	48.1	52.5
4	N/A	20.7	18.9
5	52.0	44.4	57.1
6	41.1	47.3	36.7
7	36.5	41.7	37.4
8	N/A	36.4	26.5
9	34.9	35.7	28.9
10	30.5	46.0	33.1
11	39.5	44.4	38.6
12	33.4	27.4	37.9
13	38.2	41.4	45.8
Mean	38.3	40.4	38.0
SD	7.8	8.7	11.0

N/A, Not available in the pre-planning software.

PTV in the cranial and in the caudal direction to encompass at least the 80% isodose volumes for calculation of the (high dose) DVH parameters. The bladder was delineated up to 1 cm cranial of the border of the PTV. The catheters were reconstructed on both modalities.

Dose objectives for planning were to cover at least 95% of the PTV with the prescribed dose (PD = 1.2 Gy/pulse and 28.8 Gy in total), i.e. $V_{100} \geq 95\%$ while restricting urethral dose to 140% of the PD (Ur-D0.01 $cm^3 < 140\%$) and rectal dose to 80% (Re-D2 $cm^3 < 80\%$). A dose higher than the PD was accepted for at most 2 cm^3 of the bladder (Bl-D2 $cm^3 < 100\%$).

Treatment plan evaluation

A set of three treatment plans was created for every patient: 1) CT-plan; 2) MRI-plan; and 3) CT-plan$_{MRI\text{-}contours}$. For all plans we recorded the prostate V_{100} and the other important DVH parameters for the target, i.e. prostate V_{150}, V_{200}, D_{90} and D_{100}.

Since the CT- and MRI-based treatment plans were based on different volumes but optimised with the same dwell positions available, we wanted to compare the plan quality of optimised implants. We therefore calculated three quality indices: the conformation number (CN) [9], the natural dose ratio (NDR) and the quality index (QI) [10]. These indices together define the quality of an optimised implant. The CN is calculated as: $CN = \frac{V_{100,t}}{PTV} \frac{V_{100,t}}{V_{100}}$ [9], where $V_{100,t}$ represents the target volume receiving at least the prescribed dose. These two multiplied ratios should preferably be close to one to obtain a conformal dose distribution with: 1) the smallest possible volume inside the target that is underdosed; and 2) the smallest possible volume outside the target volume that is overdosed. The NDR and QI were extracted from the natural dose volume histogram (NDVH) [10,11]. The NDR is calculated as the ratio of the natural prescription dose (NPD) to the prescribed dose, with the NPD being the optimal PD according to the dose distribution. The NPD is the isodose encompassing the implanted volume. Within this volume lies the peak dose area of the implant. The NDR indicates if the PD is chosen in accordance to the NPD and should therefore be close to one. The QI is a measure of the homogeneity of the dose distribution [10].

To assess whether the dose coverage and high dose volumes were different for the caudal and cranial part of the prostate, the delineated PTVs were divided into subvolumes, creating two new regions of interest (ROIs) for both imaging modalities. The division was based on the most central slice in the CT-based PTV. Then the MRI-based PTV was split at the same position relative to the catheters. These new ROIs and their DVHs were further analysed.

To study the radiobiological impact of dosimetric differences between the MRI-plans and CT-plans$_{MRI\text{-}contours}$, TCPs were calculated for these plans. The linear-quadratic model for incomplete monoexponential sublethal cell damage repair (LQ model) was applied [12], as elaborated in the appendix (Supplementary material online at http://informahealthcare.com/doi/abs/10.3109/0284186X.2012.744875). We did not take tumour repopulation into account, since prostatic tumours are slowly proliferating [13]. Negligible repopulation occurs if an onset time of repopulation of 34 days is assumed [14], which is close to our total treatment time of six weeks. Since the actual radiobiological parameters for the prostate are unknown, different combinations of common parameter values were used [15–17]. For the half-time of repair of sublethal damage $T_{1/2}$ an intermediate value of 1.5 hours was selected. The values for α (for single track lethality, linear dose response) were 0.03, 0.1, 0.15 and 0.3 [Gy^{-1}] and for β (double track lethality, quadratic dose response) 0.05 and 0.1 [Gy^{-2}] were selected in order to obtain α/β ratios of 0.3, 1, 1.5, 2, 3 and 6 [Gy]. Since much debate is going on and some argue that dose heterogeneity or hypoxia or modelling artefacts could have caused the low values for the α/β ratio, we also incorporated an intermediate value of 6 [18,19]. By using the clonogenic density ρ as scaling factor, average TCP for the CT-plans$_{MRI\text{-}contours}$ was set at 90%, representing the five-year biochemical non-evidence of disease (bNED) in our clinical practice [7]. The same parameter set was then applied to the MRI-plans. Inhomogeneity of the dose distribution was taken into account by calculating the TCP for every volumetric unit receiving a certain dose, using the differential DVHs. Since this is a planning study for the effect of the imaging modality on PDR brachytherapy treatment planning, the dose for EBRT (that was delivered by 3D-conformal radiotherapy) was assumed to be homogeneous throughout the target volume.

Statistics

To compare DVH parameters of the different plans, we used paired samples t-tests. The target coverage V_{100}, quality indices (NDR, CN and QI) and TCPs were compared with a non-parametric Wilcoxon signed-rank test. All statistical analyses were performed with a statistical package (IBM SPSS Statistics 19, Chicago, IL, USA).

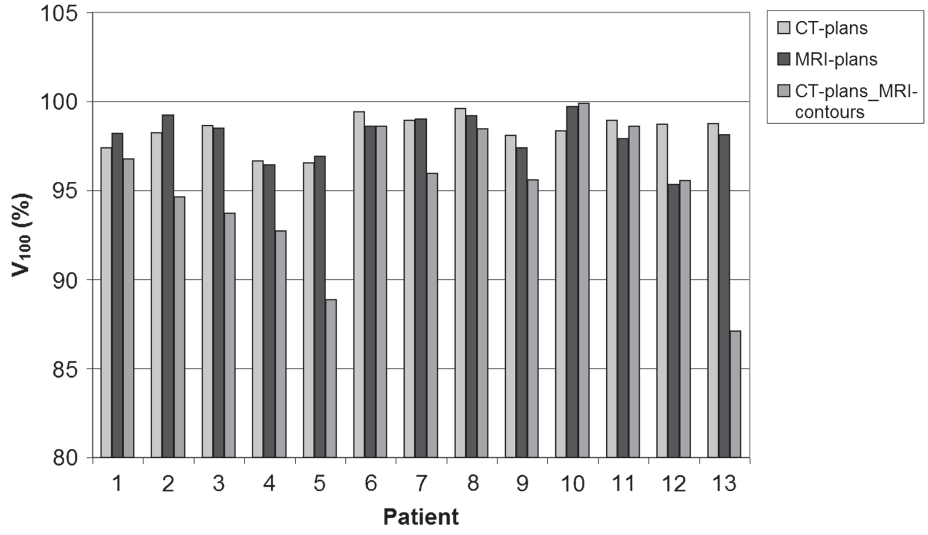

Figure 1. PTV coverage (V_{100}) for all patients of the different plans.

Results

CT-plans vs. MRI-plans

Despite the fact that the two different volumes had to be optimised with the same set of catheters, all planning objectives could be met and the differences in dosimetric parameters between CT- and MRI-plans (Figures 1 and 2) were not statistically significant. Target coverage V_{100} was always higher than 95% (CT: mean 98% with 95% CI 97.8–98.9%; MRI: mean 98% with 95% CI 97.3–98.8%) and the high dose volumes were similar and acceptable ($V_{150}<45\%$ and $V_{200}<20\%$). Between the two modalities, there was no difference in dose coverage between the two subvolumes of the prostate (mean apical V_{100} was 99% and mean basal V_{100} was 98%). Irrespective of imaging modality, the quality indices QI and CN gave comparable results for CT- and MRI-plan ($p>0.05$) (Table II). The NDR was slightly improved for the MRI-plans ($p<0.05$).

CT-plans$_{MRI\text{-}contours}$

Evaluating the CT-plans on MRI contours reduced the coverage. Mean V_{100} of CT-plans$_{MRI\text{-}contours}$ was lower than was planned on CT: 95% (95% CI 92.8–97.4%) instead of 98% ($p=0.005$). The V_{100} for all patients is shown in Figure 1. The difference in PTV coverage was mainly located at the base part of the prostate, decreasing from 98% to 95% ($p=0.007$,

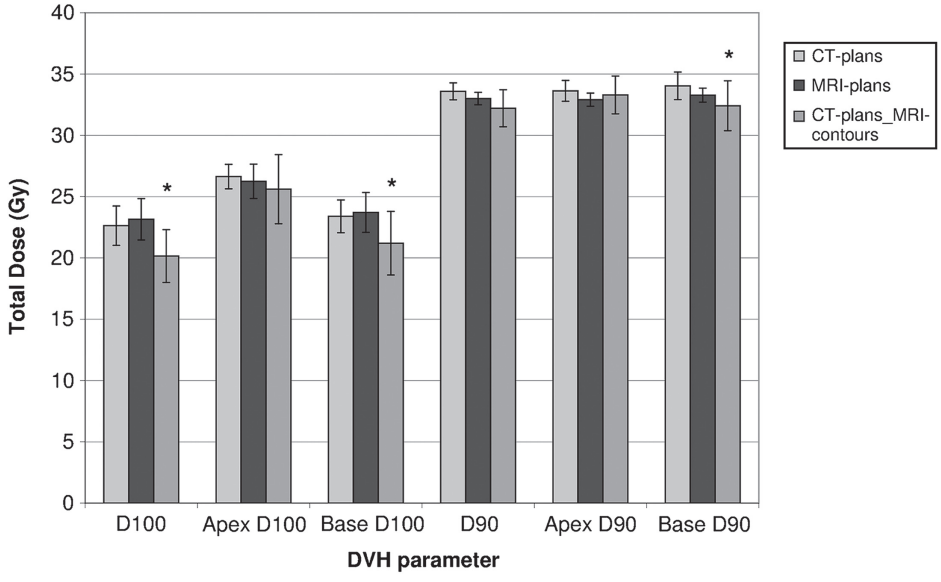

Figure 2. Dose parameters for the PTV and its two subvolumes (apical and basal part) of the different plans. Bars marked with a * give a statistically significant different result from the original CT-plans ($p<0.05$). Error bars show 95% confidence intervals.

Table II. Median and IQR (interquartile range) of the quality indices for the different plans.

	NDR		QI		CN	
	Median	IQR	Median	IQR	Median	IQR
CT-plans	1.10	1.08–1.10	1.50	1.46–1.5	0.58	0.58–0.59
MRI-plans	**1.05**	1.0–1.05	1.58	1.47–1.57	0.53	0.46–0.53
CT-plans_MRI-contours	as CT		as CT		**0.50**	0.39–0.50

For parameters in bold, the difference to the original CT-plans is statistically significant ($p < 0.05$).

95% CI 91.8–98%). D90 and D100 for the PTV and the two subvolumes are shown in Figure 2.

Differences in rectum and bladder dose of the CT-plans and CT-plans$_{\text{MRI-contours}}$ were not statistically significant. The dose to urethra volume from the CT-plans increased when evaluated on MRI-contours ($p = 0.048$). Mean dose to 0.01 cm^3 of the urethra was 2.4 Gy higher, which is almost certainly caused by small variations in contouring in combination with the large dose gradient around the urethra.

The quality indices of CT-plans$_{\text{MRI-contours}}$ and CT-plans were based on the same dose distributions. As the NDR and QI are quality indices of the plans without consideration of the target contour, they are the same. The CN showed a statistically significant deterioration for CT-plans$_{\text{MRI-contours}}$ ($p < 0.05$, Table II).

For all combinations of radiobiological parameters the mean TCP for the CT-plans$_{\text{MRI-contours}}$ was scaled at 90%, corresponding to our standard clinical practice. Deviations from 0.90 in mean TCP for CT-plan$_{\text{MRI-contours}}$ were due to rounding. Average TCP for the MRI-plans was 6–10% higher, depending on the parameters used (Table III). For the largest values for α and β the differences in TCP were most pronounced. An example of the TCPs for the different plans is shown in Figure 3.

Discussion

Taking MRI-based target delineation as our gold standard, evaluating CT-based treatment plans on MRI-contours showed that sufficient dose coverage of the target is not guaranteed when using the CT-based plan. MRI-based treatment planning resulted in improved prescription dose coverage of the actual target. We showed that MRI-based treatment planning can improve the TCP from 90% bNED at five-years to 95–99% (by 6–10%), depending on the radiobiological parameters.

The crucial difference between basing the treatment on contours created on MRI or CT is the definition of the target volume, which is more accurate when defined using MRI. Improved accuracy of target delineation will lead to improved dose coverage. Whether the use of MRI will lead to an actual improvement of tumour control remains to be established from clinical studies.

CT-plans vs. MRI-plans

Our results showed that plan quality of MRI-based dose distributions was as good as that of CT-based dose distributions. All dose objectives were met, showing that with the available dwell positions from the 12 implanted catheters, there are sufficient degrees of freedom to satisfy the constraints. No differences between the quality indices from the CT- and MRI-plans were found, only the NDR of the MRI-plans was better than the NDR of the CT-plans. The catheters were implanted into the target volume under US-guidance. Since MRI displays closer correspondence of prostate contouring to US than CT [6,20], it is likely that the implanted

Table III. TCPs from CT-plans$_{\text{MRI-contours}}$ and MRI-plans for different sets of radiobiological parameters.

				CT-plans$_{\text{MRI-contours}}$				MRI-plans				Difference		p-value
α (Gy^{-1})	β (Gy^{-2})	ρ (cm^{-3})	α/β (Gy)	Mean	SD	Min	Max	Mean	SD	Min	Max	Mean	SD	
0.03	0.05	5.E + 02	0.6	0.89	0.09	0.68	0.98	0.95	0.02	0.91	0.99	0.06	0.09	**0.019**
0.10	0.05	6.E + 04	2	0.91	0.10	0.67	0.99	0.97	0.01	0.95	1.00	0.06	0.09	**0.009**
0.15	0.05	8.E + 06	3	0.91	0.11	0.62	0.99	0.98	0.01	0.96	1.00	0.07	0.11	**0.007**
0.30	0.05	6.E + 10	6	0.89	0.17	0.43	1.00	0.99	0.01	0.96	1.00	0.09	0.16	**0.003**
0.03	0.10	6.E + 05	0.3	0.90	0.14	0.54	1.00	0.98	0.01	0.96	1.00	0.08	0.13	**0.003**
0.10	0.10	7.E + 07	1	0.90	0.16	0.46	1.00	0.99	0.01	0.97	1.00	0.09	0.16	**0.002**
0.15	0.10	2.E + 09	1.5	0.89	0.17	0.40	1.00	0.99	0.01	0.97	1.00	0.10	0.17	**0.002**
0.30	0.10	4.E + 13	3	0.90	0.20	0.30	1.00	0.99	0.01	0.98	1.00	0.10	0.20	**0.002**

Differences were tested with a Wilcoxon signed-rank test.

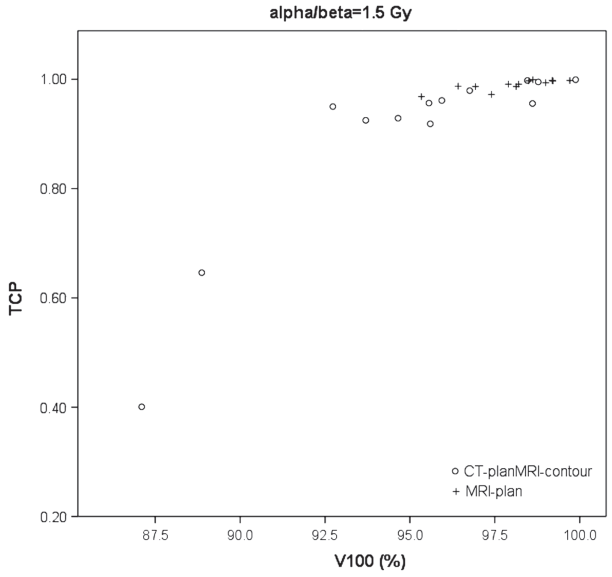

Figure 3. Example of TCPs as a function of V_{100} for one parameter sets ($\alpha = 0.15$ Gy^{-1}, and $\beta = 0.1$ Gy^{-2}). For this set, mean TCP improved 10% for MRI-plans, compared to CT-plans$_{MRI\text{-}contours}$.

volume matches the target volume defined on MRI better.

Prostate volumes

A possible limitation of this study is the subjective nature of prostate delineation. Defining the prostate on CT is hampered by the lack of visibility of internal structures and characterised by large inter- and intraobserver variability [3,5,6,20,21]. MRI displays smaller variability, but is still subject to variation in interpretation of the observer, of what to include as prostate contour [22]. However, we chose not to include a second observer in this study. In our clinical practice, the physician delineating the prostate uses the information from the US-imaging and the implantation procedure. Another observer would introduce a more random variation in the delineated volumes, not necessarily corresponding to the clinical procedure. Our physician was influenced by: 1) the knowledge of common overestimation on CT [6,23,24]; 2) US-imaging during implantation; and 3) the implant itself (visible catheters), including the implanted fiducial markers. Compensation of known overestimation has been reported by others [21,25,26], as well as the tendency to delineate the implant rather than the prostate [26–29]. This explains the small variations in prostate volume between the different modalities. Both seeds and catheters are difficult to place in the basal side of the prostate. The absence of seeds or catheters is misinterpreted as non-prostatic tissue. Instead of just overestimating the CT-based volume (as occurs in EBRT), the observer is misled by the implant. Our results reflect the differences between CT- and MRI-based treatment planning, conform clinical practice. Performing the same study at another institute can lead to different results. Although no studies exist comparing MRI to a true gold standard, there are indications that accuracy will always increase with MRI, due to smaller observer variation and uncertainties [3,5,21,26].

CT-plans$_{MRI\text{-}contours}$

Despite the small differences in prostate volume between CT and MRI, our CT-plans evaluated on the MRI-contours showed decreased dose coverage: V_{100} and D_{90} of the MRI-based PTV were statistically significantly lower than originally planned on the CT-based PTV. These parameters can be used as predictors of biochemical failure [30,31]. In our patient group, main decrease in coverage was located at the base part of the prostate, whereas most tumours are predominantly located in the peripheral zone [32]. The implications of dose coverage loss may therefore be limited. Due to the multifocal and multizonal nature of prostate carcinoma however, eradication still depends on treatment of the entire gland [32,33]. D'Amico et al. even found a significant increase in the contribution of tumour foci located in the anterior base for higher risk groups [34]. Thus far, the clinical significance of underdosage in any particular region of the prostate remains unproven.

Due to standard clinical practice for CT- and MRI-acquisition, there was a difference in patient positioning, which can affect the anatomy. However, the main effect of using knee-support is that the spacing between the prostate and the rectum is increased. The impact on PTV shape is assumed to be limited [35].

Radiobiological evaluation: TCPs

In our clinical practice, we have a five-year bNED of 90% with CT-based planning. We calculated the DVHs of CT-plans$_{MRI\text{-}contours}$ and scaled the average TCPs to 90% by varying the clonogenic density ρ. Since exact values of radiobiological parameters (α, β, ρ, $T_{1/2}$) are unknown, a spectrum of parameter values was applied (α/β: 0.3, 1, 1.5, 2, 3 and 6) [15–17]. The $T_{1/2}$ was set at a fixed value of 1.5 h. The impact of decreased dose coverage proved largely dependent on the values chosen for α and β.

This can be explained from a radiobiological point of view. Larger α/β ratios have a stronger dose-effect (steeper sigmoid curve), making the sensitivity to cold-spots larger. The difference arising from the different values for β can be explained

by the quadratic nature of this term, magnifying the impact of differences between low and high doses. When the α/β ratio is lower, the delineation errors that might be made (by using CT-based planning) may have less impact on the TCP.

Radiobiological evaluation: Dose and patient heterogeneity

In this study, TCPs were studied as a function of inhomogeneous dose [36]. Using an equivalent uniform dose (EUD) or other similar parameters would not suffice, since the aim was to study the impact of this heterogeneity on the TCP, as was done by others [36,37]. The tumour density was considered as homogeneous. While using a range of radiobiological parameters, as suggested by Carlone et al. [19], we did not incorporate the uncertainty of these parameters into our model, or inter-patient variation. The sensitivity of radiobiological parameters is increased when heterogeneous dose is taken into account [36].

Conclusion

With MRI-based treatment planning for stepping source prostate brachytherapy the chance of treatment mismatch is decreased and the TCP will be improved. Evaluating CT-plans in combination with MRI-contouring resulted not only in decreased dose conformality, but also in decreased target coverage compared to the planned coverage. This coverage loss was mainly located at the base of the prostate. Our current clinical results could improve by using MRI-based planning, considering the higher TCPs achieved with the MRI-plans. The impact of improved target delineation depends on the actual radiobiological parameters of the prostate, which are yet unknown. However, as long as the distribution of the clonogens in the target is unknown, the sensitivity of TCPs to cold-spots stresses the importance of adequate dose coverage to the entire target volume.

Declaration of interest: The authors report no conflicts of interest. The authors alone are responsible for the content and writing of the paper.

This work was supported in part by a grant from Nucletron (Veenendaal, the Netherlands).

References

[1] Zietman AL, DeSilvio ML, Slater JD, Rossi CJ, Jr., Miller DW, Adams JA, et al. Comparison of conventional-dose vs. high-dose conformal radiation therapy in clinically localized adenocarcinoma of the prostate: A randomized controlled trial. JAMA 2005;294:1233–9.

[2] Hoskin PJ, Motohashi K, Bownes P, Bryant L, Ostler P. High dose rate brachytherapy in combination with external beam radiotherapy in the radical treatment of prostate cancer: Initial results of a randomised phase three trial. Radiother Oncol 2007;84:114–20.

[3] Villeirs GM, Van VK, Vakaet L, Bral S, Claus F, De Neve WJ, et al. Interobserver delineation variation using CT versus combined CT + MRI in intensity-modulated radiotherapy for prostate cancer. Strahlenther Onkol 2005;181:424–30.

[4] Gao Z, Wilkins D, Eapen L, Morash C, Wassef Y, Gerig L. A study of prostate delineation referenced against a gold standard created from the visible human data. Radiother Oncol 2007;85:239–46.

[5] Debois M, Oyen R, Maes F, Verswijvel G, Gatti G, Bosmans H, et al. The contribution of magnetic resonance imaging to the three-dimensional treatment planning of localized prostate cancer. Int J Radiat Oncol Biol Phys 1999;45:857–65.

[6] Smith WL, Lewis C, Bauman G, Rodrigues G, D'Souza D, Ash R, et al. Prostate volume contouring: A 3D analysis of segmentation using 3DTRUS, CT, and MR. Int J Radiat Oncol Biol Phys 2007;67:1238–47.

[7] Pieters BR, Geijsen ED, Koedooder K, Blank LE, Rezaie E, van der Grient JN, et al. Treatment results of PDR brachytherapy combined with external beam radiotherapy in 106 patients with intermediate- to high-risk prostate cancer. Int J Radiat Oncol Biol Phys 2011;79:1037–42.

[8] Pieters BR, van der Grient JN, Blank LE, Koedooder K, Hulshof MC, de Reijke TM. Minimal displacement of novel self-anchoring catheters suitable for temporary prostate implants. Radiother Oncol 2006;80:69–72.

[9] van't Riet A, Mak AC, Moerland MA, Elders LH, van der Zee W. A conformation number to quantify the degree of conformality in brachytherapy and external beam irradiation: Application to the prostate. Int J Radiat Oncol Biol Phys 1997;37:731–6.

[10] Van der Laarse R, Luthmann RW. Computers in brachytherapy dosimetry. In: Joslin CAF, Flynn A, Hall EJ, editors. Principles and practice of brachytherapy using afterloading systems. London: Arnold; 2001. p. 49–80.

[11] Moerland MA, van der Laarse R, Luthmann RW, Wijrdeman HK, Battermann JJ. The combined use of the natural and the cumulative dose-volume histograms in planning and evaluation of permanent prostatic seed implants. Radiother Oncol 2000;57:279–84.

[12] Dale RG. The application of the linear-quadratic model to fractionated radiotherapy when there is incomplete normal tissue recovery between fractions, and possible implications for treatments involving multiple fractions per day. Br J Radiol 1986;59:919–27.

[13] Fowler JF. The radiobiology of prostate cancer including new aspects of fractionated radiotherapy. Acta Oncol 2005; 44:265–76.

[14] Gao M, Mayr NA, Huang Z, Zhang H, Wang JZ. When tumor repopulation starts? The onset time of prostate cancer during radiation therapy. Acta Oncol 2010;49: 1269–75.

[15] Brenner DJ, Martinez AA, Edmundson GK, Mitchell C, Thames HD. Direct evidence that prostate tumors show high sensitivity to fractionation (low alpha/beta ratio), similar to late-responding normal tissue. Int J Radiat Oncol Biol Phys 2002;52:6–13.

[16] Fowler J, Chappell R, Ritter M. Is alpha/beta for prostate tumors really low? Int J Radiat Oncol Biol Phys 2001;50: 1021–31.

[17] Wang JZ, Guerrero M, Li XA. How low is the alpha/beta ratio for prostate cancer? Int J Radiat Oncol Biol Phys 2003;55:194–203.

[18] Nahum AE, Movsas B, Horwitz EM, Stobbe CC, Chapman JD. Incorporating clinical measurements of hypoxia into tumor local control modeling of prostate cancer: Implications for the alpha/beta ratio. Int J Radiat Oncol Biol Phys 2003;57:391–401.
[19] Carlone M, Wilkins D, Raaphorst GP. Radiobiological parameters suitable for modeling individual outcomes cannot be obtained by analyzing heterogeneous population data with homogeneous tumor control model: In regard to D'Souza et al. (Int J Radiat Oncol Biol Phys 2004;58: 1540–1548). Int J Radiat Oncol Biol Phys 2005;62:298–9.
[20] Liu D, Usmani N, Ghosh S, Kamal W, Pedersen J, Pervez N, et al. Comparison of prostate volume, shape, and contouring variability determined from preimplant magnetic resonance and transrectal ultrasound images. Brachytherapy 2012; 11:284–91.
[21] Parker CC, Damyanovich A, Haycocks T, Haider M, Bayley A, Catton CN. Magnetic resonance imaging in the radiation treatment planning of localized prostate cancer using intra-prostatic fiducial markers for computed tomography co-registration. Radiother Oncol 2003;66:217–24.
[22] De Brabandere M, Hoskin P, Haustermans K, Van den Heuvel F, Siebert FA. Prostate post-implant dosimetry: Interobserver variability in seed localisation, contouring and fusion. Radiother Oncol 2012;104:192–8.
[23] Rasch C, Barillot I, Remeijer P, Touw A, van HM, Lebesque JV. Definition of the prostate in CT and MRI: A multi-observer study. Int J Radiat Oncol Biol Phys 1999;43:57–66.
[24] Roach M, Faillace-Akazawa P, Malfatti C, Holland J. Prostate volumes defined by magnetic resonance imaging and computerized tomographic scans for three-dimensional conformal radiotherapy. Int J Radiat Oncol Biol Phys 1996;35:1011–8.
[25] Prete JJ, Prestidge BR, Bice WS, Dubois DF. Comparison of MRI- and CT-based post-implant dosimetric analysis of transperineal interstitial permanent prostate brachytherapy. Radiat Oncol Investig 1998;6:90–6.
[26] Usmani N, Sloboda R, Kamal W, Ghosh S, Pervez N, Pedersen J, et al. Can images obtained with high field strength magnetic resonance imaging reduce contouring variability of the prostate? Int J Radiat Oncol Biol Phys 2011;80:728–34.
[27] Acher P, Rhode K, Morris S, Gaya A, Miquel M, Popert R, et al. Comparison of combined x-ray radiography and magnetic resonance (XMR) imaging-versus computed tomography-based dosimetry for the evaluation of permanent prostate brachytherapy implants. Int J Radiat Oncol Biol Phys 2008;71:1518–25.
[28] Petrik D, Araujo C, Kim D, Halperin R, Crook JM. Implications of CT imaging for postplan quality assessment in prostate brachytherapy. Brachytherapy 2012;11: 435–40.
[29] Aoki M, Yorozu A, Dokiya T. Results of a dummy run of postimplant dosimetry between multi-institutional centers in prostate brachytherapy with 125I seeds. Jpn J Radiol 2009; 27:410–5.
[30] Ho AY, Burri RJ, Cesaretti JA, Stone NN, Stock RG. Radiation dose predicts for biochemical control in intermediate-risk prostate cancer patients treated with low-dose-rate brachytherapy. Int J Radiat Oncol Biol Phys 2009;75:16–22.
[31] Zelefsky MJ, Kuban DA, Levy LB, Potters L, Beyer DC, Blasko JC, et al. Multi-institutional analysis of long-term outcome for stages T1-T2 prostate cancer treated with permanent seed implantation. Int J Radiat Oncol Biol Phys 2007;67:327–33.
[32] Chen ME, Johnston DA, Tang K, Babaian RJ, Troncoso P. Detailed mapping of prostate carcinoma foci: Biopsy strategy implications. Cancer 2000;89:1800–9.
[33] Merrick GS, Gutman S, Andreini H, Taubenslag W, Lindert DL, Curtis R, et al. Prostate cancer distribution in patients diagnosed by transperineal template-guided saturation biopsy. Eur Urol 2007;52:715–23.
[34] D'Amico AV, Davis A, Vargas SO, Renshaw AA, Jiroutek M, Richie JP. Defining the implant treatment volume for patients with low risk prostate cancer: does the anterior base need to be treated? Int J Radiat Oncol Biol Phys 1999;43:587–90.
[35] Steenbakkers RJ, Duppen JC, Betgen A, Lotz HT, Remeijer P, Fitton I, et al. Impact of knee support and shape of tabletop on rectum and prostate position. Int J Radiat Oncol Biol Phys 2004;60:1364–72.
[36] Lindsay PE, Moiseenko VV, Van DJ, Battista JJ. The influence of brachytherapy dose heterogeneity on estimates of alpha/beta for prostate cancer. Phys Med Biol 2003;48:507–22.
[37] D'Souza WD, Thames HD, Kuban DA. Dose-volume conundrum for response of prostate cancer to brachytherapy: Summary dosimetric measures and their relationship to tumor control probability. Int J Radiat Oncol Biol Phys 2004;58:1540–8.

Supplementary material available online

TCP calculation.